

What really happens in the Franck–Hertz experiment with mercury?

G. F. Hanne

Citation: American Journal of Physics **56**, 696 (1988);

View online: <https://doi.org/10.1119/1.15503>

View Table of Contents: <http://aapt.scitation.org/toc/ajp/56/8>

Published by the American Association of Physics Teachers

Articles you may be interested in

[New features of the Franck-Hertz experiment](#)

American Journal of Physics **74**, 423 (2006); 10.1119/1.2174033

[Franck–Hertz experiment with higher excitation level measurements](#)

American Journal of Physics **55**, 366 (1998); 10.1119/1.15174

[Elastic electron-atom collision effects in the Franck–Hertz experiment](#)

American Journal of Physics **51**, 1086 (1998); 10.1119/1.13331

[Improvement to the Franck-Hertz Experiment](#)

American Journal of Physics **27**, 645 (2005); 10.1119/1.1934948

[Comment on the Franck–Hertz experiment](#)

American Journal of Physics **44**, 302 (1998); 10.1119/1.10596

[Electron impact excitation and uv emission in the Franck–Hertz experiment](#)

American Journal of Physics **51**, 810 (1998); 10.1119/1.13123



American Association of Physics Teachers

Explore the **AAPT Career Center** – access hundreds of physics education and other STEM teaching jobs at two-year and four-year colleges and universities.

<http://jobs.aapt.org>



What really happens in the Franck-Hertz experiment with mercury?

G. F. Hanne^{a)}

The University of Oklahoma, Department of Physics and Astronomy, 440 West Brooks, Norman,
Oklahoma 73019

(Received 17 February 1987; accepted for publication 15 October 1987)

Recent studies using spin-polarized electrons have revealed the role that various interactions play in inelastic collisions of slow electrons with complex atoms. It has been shown that electron exchange and resonances (temporarily negative compound ion states) strongly influence the excitation cross sections of the first excited states of mercury very close to excitation thresholds. The particular result obtained in the Franck-Hertz experiment is determined by the magnitude of the excitation cross sections involved and depends on the geometrical design of the tube.

I. INTRODUCTION

The electron-mercury collision experiment of Franck and Hertz,¹ for which they won the Nobel Prize in 1925, is one of the key experiments that helped to establish modern atomic theory. It shows that atoms can absorb energy only in quantum portions confirming Bohr's postulates. Due to its simplicity and the clear-cut experimental result—which facilitated its explanation by Franck and Hertz—it is often demonstrated in classes and cited in most textbooks of modern physics. However, this experiment would not show such clear-cut results if there were not special circumstances, which have been revealed only very recently by studies using modern experimental and theoretical techniques. The purpose of the present article is to review and interpret some of these recent studies and to show that the Franck-Hertz experiment contains much more interesting collision physics than is usually assumed. A real understanding of the outcome of this apparently simple experiment requires a detailed knowledge of the basic collision processes by which it is governed.

II. THE TEXTBOOK EXPLANATION OF THE FRANCK-HERTZ CURVE

Figure 1 shows a schematic diagram of a tube with which the experiment is usually performed and the result of the experiment. Electrons are emitted from the cathode with nearly zero kinetic energy. They gain kinetic energy in traveling toward the control grid, which is positive relative to the cathode by U volts. In transit, they collide with mercury atoms in the tube and lose energy. Electrons that reach the grid with kinetic energy of 1.5 eV or more will be able to reach the anode and be included in the measured current I_c . Electrons with an energy of less than 1.5 eV at the control grid will be unable to reach the anode and will fall back to the control grid. These are not included in the measured current I_c . Franck and Hertz originally thought that the peak spacing in the curve they obtained had to do with the ionization potential of mercury but, later, they gave the correct explanation, which in a modern textbook,² reads: "... the peaks occurring at a spacing of about 4.9 eV. The first dip corresponds to electrons that lose all their kinetic energy after one inelastic collision with a mercury atom, which is then left in an excited state. The second dip corresponds to those electrons that suffered two inelastic collisions with two mercury atoms, losing all their kinetic energy and so on. The excited mercury atoms return to their ground state by emission of a photon, according to

$Hg^* \rightarrow Hg + h\nu$ with $h\nu = E_2 - E_1$. From spectroscopic evidence, we know that mercury vapor, when excited, emits radiation whose wavelength is 2536 Å, corresponding to a photon energy $h\nu$ equal to 4.89 eV. Radiation of this wavelength is observed coming from the mercury vapor during the passage of the electron beam through the vapor. . . ."

This simple explanation is correct in principle. However, a deeper insight into the problem raises two questions: Is the observed energy loss the result of a simple inelastic collision and why is the energy loss about 4.9 eV? The first excited state in mercury corresponds to an energy loss of 4.67 eV, as indicated in Fig. 2, which is a simplified energy-level scheme of the first excited states of mercury in which the hyperfine structure due to nuclear spin has been neglected. These questions will be discussed, and it will be shown that the observed peak separation depends on the geometry of the tube and the Hg vapor pressure and is mainly, but not solely, related to the 4.89-eV transition. Thus students and instructors should not worry about results that show a peak spacing in the Franck-Hertz curve that deviates from 4.89 V by a few tenths of a volt.

III. ELECTRON EXCHANGE IS A SIGNIFICANT EXCITATION MECHANISM

The first excited states in mercury are known to have mainly triplet character (cf. Fig. 2), i.e., the dominating

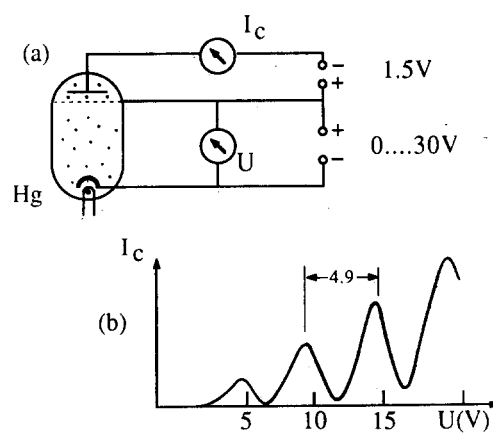


Fig. 1. (a) Schematic diagram of the Franck-Hertz experiment; (b) typical curve recorded in a Franck-Hertz experiment with mercury.

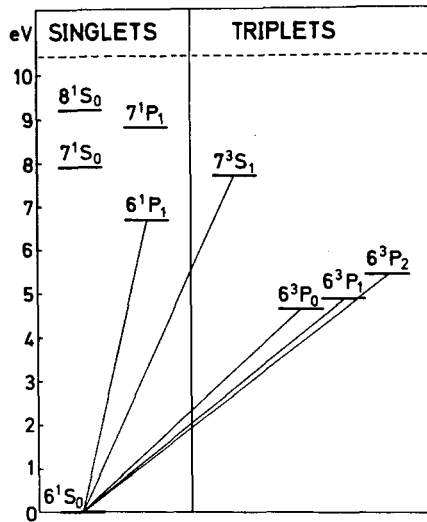
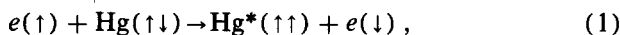


Fig. 2. Simplified energy level scheme of the lowest states of the mercury atom (hyperfine structure neglected).

configuration consists of two valence electrons in $6s6p$ orbitals giving a total P state where the spins are coupled to a total spin with quantum number $S = 1$ (multiplicity $2S + 1 = 3$). The spin-orbit interaction splits this configuration into three states $6^3P_{0,1,2}$ with total angular momentum quantum numbers $J = 0, 1, 2$. The states with $J = 0, 2$ are metastable, i.e., they cannot decay into the 6^1S_0 ground state because dipole emission is forbidden for transitions with $\Delta S \neq 0$, and, in particular, $J = 0, 2 \rightarrow J = 0$. The strong spin-orbit interaction within the mercury atom results in a small but significant singlet admixture to the 6^3P_1 state (i.e., this state is not a pure triplet state) allowing the well-known optical transition $6^3P_1 - 6^1S_0$ (254-nm intercombination line).³

It is expected that the $6^1S \rightarrow 6^3P$ electron impact excitation is dominated by electron exchange collisions leading to reactions such as⁴



where the arrows denote the electron spin orientations with respect to a given axis. That processes like (1) dominate the excitation of $\text{Hg}^*(\uparrow\uparrow)$ states at low energies has been demonstrated more than ten years ago in a special version of the Franck-Hertz experiment.⁴ According to reaction (1) the spin orientation of the “scattered” electron will be changed in such a collision. Initially polarized electrons with polarization P were used and the polarization P' of “scattered” electrons was measured. Any value $P'/P < 1$ is direct evidence of exchange provided that other interactions that could change the spin orientation do not exist.

A schematic diagram of the apparatus used is shown in Fig. 3(a). Transversely polarized electrons resulting from elastic scattering by a mercury vapor beam⁶ pass through a filter lens that removes inelastically scattered electrons. The electrons are then decelerated and focused onto a second mercury vapor beam. From the electrons scattered in the forward direction, those which have excited a certain atomic state and lost the excitation energy are selected by a cylindrical mirror analyzer. The transverse spin polarization P' of the inelastically scattered electrons is measured in a Mott detector⁶ after acceleration to 120 keV. The initial

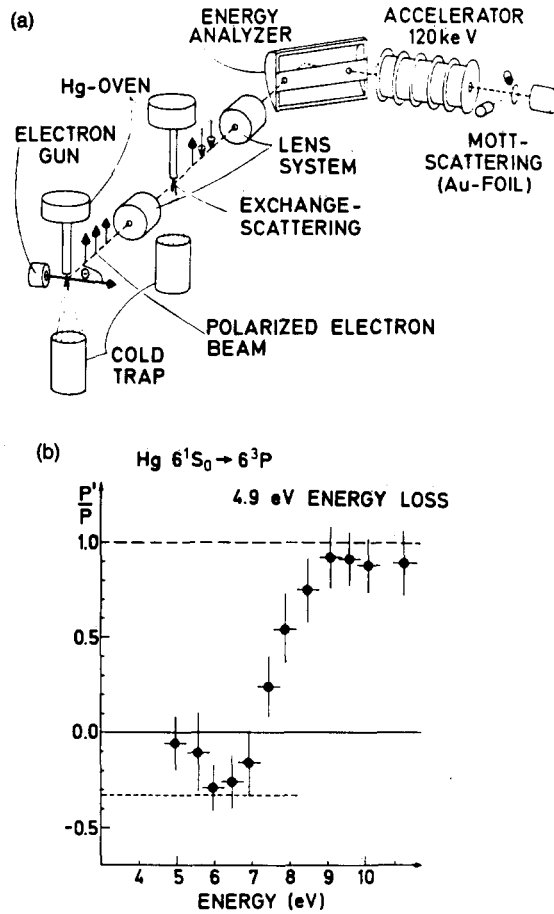


Fig. 3. (a) Schematic diagram of the apparatus for direct observation of exchange collisions; (b) measured ratio P'/P versus energy for electron impact excitation of mercury with a mean energy loss 4.9 eV.

polarization P is measured by tuning the electron spectrometer to zero energy loss.

Figure 3(b) shows the measured ratio P'/P for excitation of the 6^3P states at a mean energy loss of 4.9 eV. This is the energy loss that occurs most frequently in the Franck-Hertz experiment. Clearly $P'/P < 1$ close above the excitation threshold indicates that electron exchange is a significant collision mechanism. As the probability for exchange decreases for electron energies above 9 eV, P'/P increases and approaches a value of 1 above 9 eV. Above 9 eV, simple inelastic collisions without a change of spin orientation dominate by the singlet admixture of the 6^3P_1 state.⁴

With this experiment, the importance of electron exchange has been demonstrated only for forward scattering angles. When the scattering angle is large, the spin-orbit interaction due to the motion of the scattered electrons in the field of the atomic nucleus may be significant.⁶ This prevents a straightforward interpretation of observed “spin flips” as being due only to exchange collisions. Recent experimental and theoretical studies of spin effects in inelastic electron-mercury collisions, however, have shown that exchange collisions are very probable also at large scattering angles.⁷⁻¹³ It is beyond the scope of the present article to discuss these studies and the interpretation of their results. The interested reader is referred to the original publications cited above. These investigations, however, show also another feature that significantly influences the probability

for the energy losses observed in a Franck-Hertz curve. This will be discussed in Sec. IV.

IV. FORMATION OF TEMPORARILY NEGATIVE ION STATES: RESONANCES

There are several experimental procedures that yield cross sections for the excitation of the resolved $6^3P_{0,1,2}$ fine-structure states. The simplest method seems to collect the inelastically scattered electrons. But since the scattered electrons lose nearly all their kinetic energy very close to the excitation threshold, these slow electrons are difficult to detect. In addition, such a measurement would require an integration over all scattering angles.

Very good results have been obtained in experiments where the excited metastable ($6^3P_{0,2}$) mercury atoms were detected with channeltrons.^{14,15} However, above the threshold for excitation of the 6^3P_2 state (5.46 eV) no discrimination between the 6^3P_0 and 6^3P_2 metastable states is possible with this method.

Such a discrimination was feasible in an experiment¹⁶ where fluorescence emission ($7^3S_1 - 6^3P_{0,1,2}$) was induced by laser light tuned to the $6^3P_0 - 7^3S_1$ or $6^3P_2 - 7^3S_1$ transitions after the 6^3P_0 and 6^3P_2 states have been excited by electron impact. The intensity of this fluorescence is a measure for the excitation cross section of the particular metastable state under study.

The cross section for excitation of the 6^3P_1 state cannot be obtained with the two methods because of the relatively short lifetime (120 ns) of this state. However, the intensity of the fluorescence light (254 nm) from the $6^3P_1 - 6^1S_0$ optical decay just mentioned is a measure of the excitation cross section of direct electron impact excitation.^{17,18}

Recently, these excitation cross sections have been calculated for the first time using an R matrix close-coupling method.¹⁹ As a summary of all experimental and theoretical results, the behavior of the cross sections for excitation of the lowest ($6^3P_{0,1,2}$) mercury states is shown in Fig. 4 for energies from the excitation thresholds up to 6 eV. The relative as well as the absolute values of the cross sections are uncertain by 30% because of the lack of precise absolute measurements.

Each of the three curves exhibits a sharp increase above the excitation thresholds and two curves exhibit an additional sharp or broad maximum before decreasing at ener-

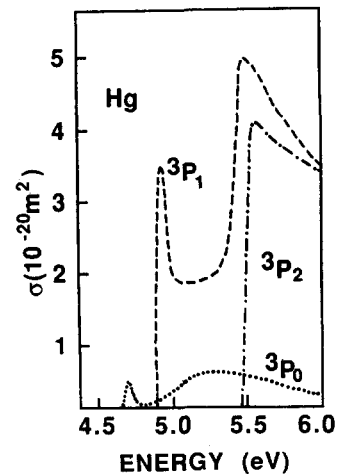


Fig. 4. Cross sections for electron impact excitation of mercury states 6^3P_0 (energy loss 4.67 eV), 6^3P_1 (energy loss 4.89), and 6^3P_2 (energy loss 5.46 eV) versus energy. These data are estimates taken from various measurements and calculations in the literature and are uncertain up to 30% because of the lack of precise absolute measurements.

gies above 5.5 eV. The maxima occur at 4.7, 4.92, 5.2, and 5.59 eV. At these energies, there is a significant probability for the incident electron to be captured temporarily by the atom ("resonance") to form a negative ion. These negative ions live for about 10^{-13} s or less if the widths of the peaks are 20 meV or more. A mercury atom finally may be found in the ground state or in one of the excited states provided that energy conservation permits such a decay. The classification of these Hg^- resonance states has been controversial since their first observation by Kuyatt *et al.*²⁰ Fano and Cooper²¹ suggested that these resonances should have the Hg^- ($6s6p^2$) configuration. Several classification schemes had been suggested that differed particularly in the assignment of quantum numbers to the structure of 4.92 eV just above the 6^3P_1 threshold. Furthermore, not all of the compound ion states that were expected by Fano and Cooper and Heddle²² had been fully confirmed. An example of a recent experiment that helped clarify the situation is the investigation of the circular polarization of the 254-nm fluorescence emission excited by polarized electrons.¹⁸

Figure 5 is a schematic diagram of the apparatus. A GaAs photocathode in ultrahigh vacuum is irradiated by circularly polarized laser light with the result that longitudinally polarized electrons are emitted.²³ After deflection of the electrons through 90°, their polarization is rotated by two magnetic coils through 90° to be perpendicular to the xz plane. The electrons then pass through a differential pumping stage where they are again deflected through 90°. A lens system focuses the polarized electron beam onto the mercury beam target. At the target, the electrons are polarized along the y direction. Some of the mercury atoms are excited by electron impact. A photon analyzer system measures the circular polarization of the $6^3P_1 - 6^1S_0$ resonance line (254 nm) (by a $\lambda/4$ plate and a linear polarization analyzer) as a function of collision energy between 4.5 and 7 eV. The photon analyzer detects photons that are emitted in the direction of the electron spin polarization.

The result is shown in Fig. 6. The significance of the result lies in the fact that around 5.2 eV the circular polarization is negative. A formal analysis¹⁸ shows that nonresonant exchange collisions result in a positive circular polarization. However, the temporary formation of a Hg^-

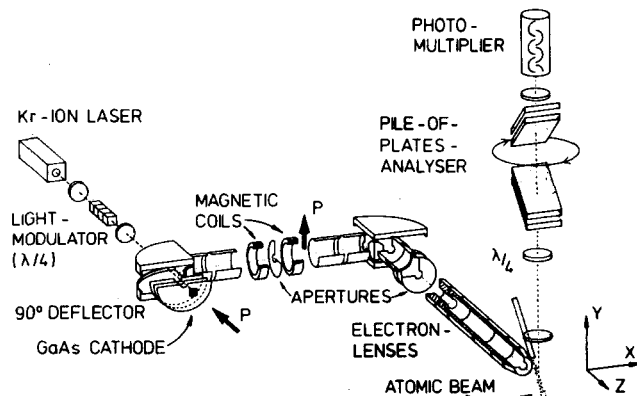


Fig. 5. Schematic diagram of the apparatus used by Wolcke *et al.*¹⁸ for measuring the circular polarization of 254-nm fluorescence light emitted after electron impact excitation of mercury atoms with polarized electrons.

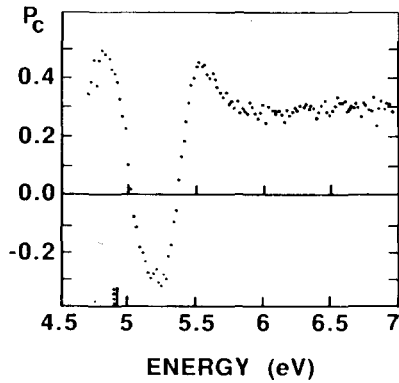


Fig. 6. Circular polarization $P_c = (I^+ - I^-)/(I^+ + I^-)$ versus energy for 254-nm fluorescence light emitted after electron impact excitation of mercury with polarized electrons. Here, I^+ and I^- are the intensities of light transmitted by a filter for photons with positive and negative helicity (or left and right circular polarization), respectively.

ion state with total angular momentum $J = \frac{3}{2}$ results in a negative value, whereas a negative ion state with $J = \frac{5}{2}$ leads to a positive value. This helped to establish the existence of a broad $J = \frac{3}{2}$ resonance that is invisible in the 6^3P_1 excitation cross section but was later shown clearly in the 6^3P_0 excitation cross section (cf. Fig. 4).¹⁶ The most probable classification scheme of the Hg^- ($6s6p^2$) resonances is (Table I)^{18,24}: $^4P_{1/2}$ (4.55 eV, seen only in the elastic cross section),^{25,26} $^2P_{3/2}$ (4.7 eV seen in the 6^3P_0 cross section), $^4P_{5/2}$ (4.92 eV seen in the 6^3P_1 cross section, but not in the 6^3P_0 cross section as decay in this state is strongly suppressed because of the centrifugal forces of the high orbital angular momentum that the emerging electron must carry away¹⁶), $^2D_{3/2}$ (5.2 eV, seen as a broad maximum in the 6^3P_0 curve, invisible in the 6^3P_1 curve) and $^2D_{5/2}$ (5.5 eV seen in both 6^3P_1 and 6^3P_2 curves).

How does the behavior of the cross sections shown in Fig. 4 influence the outcome of the Franck-Hertz experiment?²⁷

V. THE SHAPE OF THE FRANCK-HERTZ CURVE DEPENDS ON THE TUBE DESIGN

One of the two questions raised in Sec. II has already been answered by Secs. III and IV: The energy loss obtained by recording the Franck-Hertz curve is not the result of simple inelastic collisions where the electrons lose all their kinetic energy, it is a complicated process where exchange collisions and the formation of short-lived Hg^- -ion states dominate.

Table I. Classification of Hg^- ($6s6p^2$) states^{18,24}

Configuration	Energy (eV)	Visible in the cross section for
$^4P_{1/2}$	4.55	elastic scattering
$^4P_{3/2}$	4.70	elastic scattering, 6^3P_0 excitation
$^4P_{5/2}$	4.92	elastic scattering, 6^3P_1 excitation
$^2D_{3/2}$	~5.2	6^3P_0 excitation
$^2D_{5/2}$	5.50	elastic scattering, $6^3P_{1,2}$ excitation

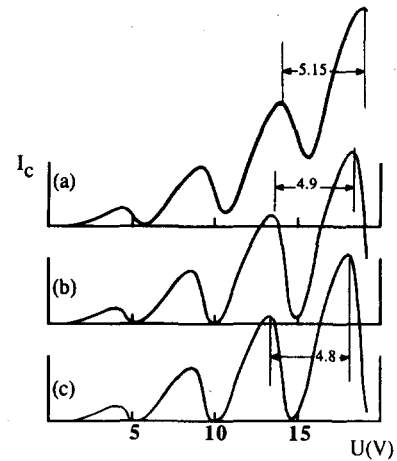


Fig. 7. (a) Simulated Franck-Hertz curve for $p_{\text{Hg}} \times d \approx 4$ mbar cm, where p_{Hg} and d are mercury pressure and distance cathode-anode in the tube, respectively; (b) same for $p_{\text{Hg}} \times d \approx 20$ mbar cm with which the Franck-Hertz experiment usually runs, giving the most obtained peak spacing of 4.9 V; (c) same for $p_{\text{Hg}} \times d \approx 100$ mbar cm.

The second question is: Why is the observed energy loss approximately 4.9 eV instead of 4.67 eV, the energy of the first excited state (6^3P_0)? The answer can be found by examination of Fig. 4. As an electron passes from the cathode to the control grid it gains kinetic energy. At a given point in the transit, the kinetic energy is proportional to the product of the potential difference times the fraction of the electrode separation that is traveled minus the kinetic energy losses due to prior collisions. Whenever the kinetic energy reaches 4.67 eV excitation of the 6^3P_0 state is possible, but only a few electrons give up 4.67 eV of kinetic energy by exciting the 6^3P_0 state due to its small cross section with the result that the electrons have a large mean free path. Those remaining continue to gain kinetic energy and reach 4.9 eV or more where many of these electrons excite the 6^3P_1 state as it has a high cross section above 4.9 eV. Some electrons do not yet even lose their kinetic energy and continue toward the control grid and gain as much as 5.5 eV or more, enough to excite the 6^3P_2 state. The tendency for a larger fraction of the electrons to gain enough kinetic energy to excite the 6^3P_1 and 6^3P_2 states increases with decreasing mercury vapor pressure and depends on the tube design as explained in the next paragraph.

That the peak spacing in the Franck-Hertz curve depends on the conditions under which the experiment is performed is demonstrated by a model calculation simulating the outcome of a Franck-Hertz experiment. Results are shown in Fig. 7. These calculations should not be taken too seriously because of very crude approximations made: homogeneous electric field, isotropic differential excitation cross sections, simple Maxwellian electron-energy distribution, neglect of repeatedly elastic collisions that lead to small energy losses as obtained in swarm experiments and other simplifications. The important inputs of these calculations are the mercury vapor pressure p_{Hg} , the distance d between cathode and anode, and the cross sections shown in Fig. 4. These inputs determine the relationship between mean free path and energy gain within the mean free path. Curve 7(b) represents the situation most nearly realized leading to a peak spacing in the Franck-Hertz curve of

about 4.9 V. If the product $p_{Hg} \times d$ is five times larger the spacing is calculated to be only 4.8 V [Fig. 7(c)] indicating that in this case the 6^3P_0 state has been excited (energy loss 4.67 eV) with a significant probability in addition to the 6^3P_1 state. If, on the other hand, the product $p_{Hg} \times d$ is five times smaller than normal a considerable number of electrons may even gain 5.5 eV to excite the 6^3P_2 states, which results in a peak spacing of 5.15 V or more [cf. Fig. 7(a)].

ACKNOWLEDGMENT

I am indebted to Professor R. St. John for reading the manuscript and making valuable suggestions.

^{a)} Present address: Westf. Wilhelms-Universität, Physikal. Institut, D-4400 Münster, Germany

¹J. Franck and G. Hertz, Verh. Deutsche Phys. Ges. **16**, 457 (1914).

²B. Alonso and A. Finn, *Introduction to Physics*, Vol. III (Addison-Wesley, Reading, MA, 1971).

³A Lurio, Phys. Rev. A **140**, 1505 (1965).

⁴G.F. Hanne and J. Kessler, J. Phys. B **9**, 805 (1976).

⁵The degree of polarization is defined by $P = (N\uparrow - N\downarrow)/(N\uparrow + N\downarrow)$, where $N\uparrow$ and $N\downarrow$ are the numbers of electrons with spin parallel and antiparallel to a preferential direction.

⁶J. Kessler, *Polarized Electrons* (Springer-Verlag, Berlin, 1985), 2nd ed.

⁷K. Bartschat, G.F. Hanne, A. Wolcke, and J. Kessler, Phys. Rev. Lett. **47**, 997 (1981).

⁸G.F. Hanne, Phys. Rep. **95**, 95 (1983).

⁹K. Bartschat, K. Blum, P.G. Burke, G.F. Hanne, and N.S. Scott, J. Phys. B **17**, 3797 (1984).

¹⁰K. Bartschat, D.H. Madison, and G.F. Hanne, J. Phys. B **18**, 1847 (1985).

¹¹H. Borgmann, J. Goeke, G.F. Hanne, J. Kessler, and A. Wolcke, J. Phys. B **20**, 1619 (1987).

¹²K. Bartschat and D.H. Madison, J. Phys. B **20**, 1609 (1987).

¹³A. Wolcke, C. Hoelscher, E. Weigold, and G.F. Hanne, J. Phys. E **20**, 299 (1987).

¹⁴L. Koch, T. Heindorff, and E. Reichert, Z. Phys. A **316**, 127 (1984).

¹⁵D.S. Newman, M. Zubek, and G.C. King, J. Phys. B **18**, 985 (1985).

¹⁶G.F. Hanne, V. Nickich, and M. Sohn, J. Phys. B **18**, 2037 (1985).

¹⁷T.W. Ottley and H. Kleinpoppen, J. Phys. B **8**, 621 (1975).

¹⁸A. Wolcke, K. Bartschat, K. Blum, H. Borgmann, G.F. Hanne, and J. Kessler, J. Phys. B **16**, 639 (1983).

¹⁹N.S. Scott, P.G. Burke, and K. Bartschat, J. Phys. B **16**, 361 (1983).

²⁰C.E. Kuyatt, J.A. Simpson, and S.R. Mielczarek, Phys. Rev. A **138**, 385 (1965).

²¹U. Fano and J.W. Cooper, Phys. Rev. A **138**, 400 (1965).

²²D.W.O. Heddle, J. Phys. B **8**, 33 (1975).

²³D.T. Pierce, R.J. Celotta, G.C. Wang, W.N. Unertl, A. Galejs, C.E. Kuyatt, and S.R. Mielczarek, Rev. Sci. Instrum. **51**, 478 (1980).

²⁴D.W.O. Heddle, J. Phys. B **11**, 711 (1978).

²⁵P.D. Burrow and J.A. Michejda, Int. Symp. on Electron and Photon Interactions with Atoms, Stirling, Book of Abstracts (1974).

²⁶K. Albert, C. Christian, T. Heindorff, E. Reichert, and S. Schön, J. Phys. B **10**, 3733 (1977).

²⁷D. W. O. Heddle, Contemp. Phys. **17**, 443 (1976).

Dielectric slab in a parallel-plate condenser

Constantino A. Utreras-Díaz

Departamento de Física, F. C. F. M., Universidad de Chile, Casilla 487-3, Santiago, Chile

(Received 29 April 1987; accepted for publication 5 October 1987)

The problem of a dielectric slab inside a parallel-plate capacitor is considered from the point of view of a simple force calculation. The usual method of presenting this problem, found in most textbooks, is via energy considerations. The method presented here allows corrections to the well-known result to be obtained.

Consider the problem of calculating the force exerted by a parallel-plate condenser, set at potential V_0 , over a dielectric slab pushed halfway into the gap of the condenser. This problem is an elementary one, discussed in most textbooks. The discussions found there are usually expressed in terms of the energy of the system. The force is calculated by differentiating the energy with respect to the distance "t" that the plate has penetrated into the condenser gap. A different point of view has been presented by Margulies¹; in his work he discusses the problem in terms of the inhomogeneities of the field, arguing that the force on the dielectric is entirely due to the "tail" of the field in the region outside the plates. In this article, I calculate the forces by examining the surface charges on the conductor and dielectric.

The geometry of the problem is as shown in Fig. 1, which depicts a condenser made of parallel plates of sides "a" and "b," separated by a distance "d." A dielectric slab of per-

mittivity ϵ , and the same dimensions is introduced a distance "t" into the gap.

As it is shown in most textbooks on electricity,² a polarized dielectric can be replaced by an equivalent combination of "real" and "polarization" charges in such a way that the electric field is generated by both kinds of charge. In general, this approach is not very useful in actual calculations, and one calculates the displacement vector \mathbf{D} . In this case, however, the charge distributions, both real and polarization, are known, at least approximately. Assuming a potential difference V_0 , the field between the plates is $\sim V_0/d$; therefore, the surface charge density on the upper conducting plates is, in mks units,

$$\sigma(x,z) = \begin{cases} \epsilon_0 V_0/d, & \text{for } 0 < x < c, \quad 0 < z < a, \\ \epsilon V_0/d, & \text{for } c < x < b, \quad 0 < z < a, \end{cases} \quad (1)$$

the charge density on the lower plate is $-\sigma(x,z)$. Calculu-